Al-Khwarizmi Engineering Journal

Al-Khwarizmi Engineering Journal, Vol. 7, No. 4, PP 27-40 (2011)

Control on a 2-D Wing Flutter Using an Adaptive Nonlinear Neural Controller

Mauwafak A. Tawfik* Mohammed I. Mohsin* Hayder S. Abd Al-Amir**

** Department of Mechanical Engineering /University of Technology*

*** Department of Mechanical Engineering /Institute of Technology*

Email: has_04@yahoo.com

(Received 23 February 2011; Accepted 6 July 2011)

Abstract

An adaptive nonlinear neural controller to reduce the nonlinear flutter in 2-D wing is proposed in the paper. The nonlinearities in the system come from the quasi steady aerodynamic model and torsional spring in pitch direction. Time domain simulations are used to examine the dynamic aero elastic instabilities of the system (e.g. the onset of flutter and limit cycle oscillation, LCO). The structure of the controller consists of two models :the modified Elman neural network (MENN) and the feed forward multi-layer Perceptron (MLP). The MENN model is trained with off-line and on-line stages to guarantee that the outputs of the model accurately represent the plunge and pitch motion of the wing and this neural model acts as the identifier. The feed forward neural controller is trained off-line and adaptive weights are implemented on-line to find the flap angles, which controls the plunge and pitch motion of the wing. The general back propagation algorithm is used to learn the feed forward neural controller and the neural identifier. The simulation results show the effectiveness of the proposed control algorithm; this is demonstrated by the minimized tracking error to zero approximation with very acceptable settling time even with the existence of bounded external disturbances.

Keywords: *Adaptive Nonlinear Control, Flutter, Nonlinear system, Neural Network.*

1. Introduction

The performance of aircraft is often limited by adverse aero elastic interactions such as flutter. Flutter is defined as a dynamic instability of a flight vehicle associated with the interaction of aerodynamic, elastic, and inertial forces. If flutter can be controlled at cruise speeds, lighter wings can be designed and consequently more efficient airplanes. It is therefore, in the aircraft designer's best interest to design innovative ways in which flutter can be controlled without making the resulting structure too heavy The nonlinear flutter models behavior is close to the systems in nature. However, the control on the flutter resulting from nonlinear models is not an easy task and need more development. In reality nonlinearities may be presented in various forms [1,2] .Recently, many researches in this field proposed different nonlinear flutter controllers, where the linear controller could not effectively suppress the flutter [3]. Palaniappan, et al. [4] developed a feedback algorithm for the control of nonlinear flutter. The actuators are jets in the walls through which there is a small mass flow, either by way of blowing or suction. Afkhami and Alighanbair [5] presented nonlinear controller to control flutter. Integral-input-to-state stability concept is utilized for the construction of a feedback controller. Haiwei and Jinglong [6] proposed the robust flutter analysis of a nonlinear 2-D wing section with structural and aerodynamic uncertain using μ-method. The parametric uncertainty was adopted to describe the uncertainties in structure and aerodynamics. The nonlinear system was linearized at equilibrium point and μ analysis is performed for a set of values of flow velocities to generate the lower and upper bounds of robust flutter speed. For a typical section with a

structural nonlinearity, Zeng and Singh [7] have derived a nonlinear adaptive control based on the model reference adaptive control theory. The system design was based on an output feedback method that eliminates the requirement for full state reconstruction. However, the derived control system exhibits somewhat larger flap deflections in simulations than others.

The neural networks were introduced in aero elastic field as nonlinear controller or flutter prediction device. Melin and Castillo[8] combined adaptive model-based control using neural networks with the method for modeling using fuzzy logic, and fractal theory to obtain a new hybrid neuro-fuzzy-fractal method for the control of nonlinear dynamic aircraft. The adaptive controller can be used to control chaotic and unstable behavior in aircraft systems. Chen, et al. [9] presented an approach using artificial neural networks (ANN) algorithm for predicting the flutter derivatives of rectangular section models without wind tunnel tests. The database of flutter derivatives was identified from a back-propagation (BP) ANN model that is built using experimental dynamic responses of rectangular section models in smooth flow as the input/output data. These limited sets of database are employed as input/output data to establish a prediction ANN frame model to further predict the flutter derivatives for other rectangular section models without conducting wind tunnel tests. The results presented indicate that this ANN prediction scheme works reasonably well.

The contribution of the present work is the utilization of a relatively simple approximation neural network to identify the posture of the non linear 2-D wing system and to design an adaptive nonlinear neural controller.

2. Method of Analysis

2.1. Two Dimensional Aero elastic Wing Model

The 2-D aero elastic wing section is shown in Figure (1). The governing equations of motion are provided in [5] and are given as:

$$m\ddot{h} + mx_a b\ddot{\alpha} + c_h \dot{h} + k_h h = -L$$

$$I\ddot{\alpha} + mx_a b\ddot{h} + c_\alpha \dot{\alpha} + k_\alpha(\alpha)\alpha = M \qquad \ldots(1)$$

where h is the plunge displacement and α is the pitch angle. In Eq. (1), m is the mass of the wing; b is the semichord of the wing; I is the moment of inertia; x_α is the nondimensionalized distance of the center of mass from the elastic axis; k_h is plunge stiffness coefficient; $k_\alpha(\alpha)$ is nonlinear pitch stiffness c_h and c_α are plunge and pitch damping coefficients, respectively; L and M are the aerodynamic lift and moment. In the present work, the nonlinear quasi steady aerodynamic model including stall effect [10] and flap angle effect [5] is as follow

$$L = rU^2 bC_{L\alpha}(\alpha_{eff} - c_3\alpha_{eff}^3) + rU^2 bC_{Lb1}b_1 + rU^2 bC_{Lb2}b_2$$

$$M = rU^2 b^2 C_{m\alpha}(\alpha_{eff} - c_3\alpha_{eff}^3) + rU^2 b^2 C_{mb1}b_1 + rU^2 b^2 C_{mb2}b_2 \qquad \ldots(2)$$

where ρ is the air density, U is the flow velocity, and $C_{L\alpha}$ and $C_{m\alpha}$ are the lift and moment coefficients. $C_{L\beta}$ and $C_{m\beta}$ are the lift and moment coefficients per flap angle. β_1 and β_2 are flap angles. c_3 is a nonlinear parameter associated with stall model. α_{eff} is the effective angle of attack defined by

$$\alpha_{eff} = \alpha + \dot{h}/U + (0.5\text{-}d)b\dot{\alpha}/U \qquad \ldots(3)$$

where d is the non dimensional distance from the mid chord to the elastic axis. Parameter c_3 is defined as follow for NACA 0012 airfoil (a symmetric wing section by National Advisory Committee for Aeronautics),

$$c_3 = 0.00034189(180/\pi)3/C_{L\alpha} \qquad \ldots(4)$$

This aerodynamic model is valid for $\alpha_{\text{eff}} \in (-11, 11)$ degree.

The function $k_\alpha(\alpha)$ is considered as a polynomial given by [10]

$$k_\alpha(\alpha) = k_{\alpha1} + k_{\alpha2}\alpha + k_{\alpha3}\alpha^2, \qquad \ldots(5)$$

where $k_{\alpha j}$, $j = 1, 2, 3$ are constants.

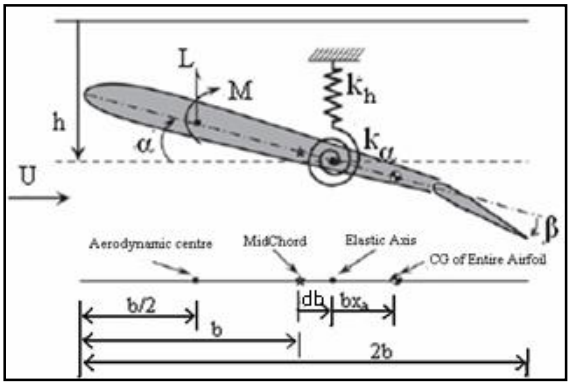

Fig.1. Two-Dimensional Aero elastic Model.

2.2. Nonlinear Flutter analysis

The proposed nonlinear controller must work in the unstable region .Time domain simulation is used to examine the dynamic aeroelastic instabilities of the system (e.g. the onset of flutter and limit cycle oscillation (LCO)) [11].The simulation is performed by solving eqs (1-5) and using Runge Kutta method for different velocities and initial conditions.It was found that LCO appears at U=9.9m/sec and never appear at speed less than what ever the initial conditions. Therefore the flutter speed is 9.9m/sec and the proposed nonlinear controller must give a good performance at speed higher than that value (unstable region).

Figure (2) shows the plunge *h* and pitch angle α responses at speed 9.8m/sec while the responses at speed 9.9m/sec are shown in the figure (3) The time responses of the plunge *h* and pitch angle α corresponding to the uncontrolled system at U=30m/sec, and 40m/sec are shown in figure (4).Clearly, the system responses exhibit LCO behaviour. It is clear that the amplitudes of LCO increase with the velocity. The function of controller is to reduce amplitudes of LCO at short settling time in order to eliminate the risk of damage of wing structure.

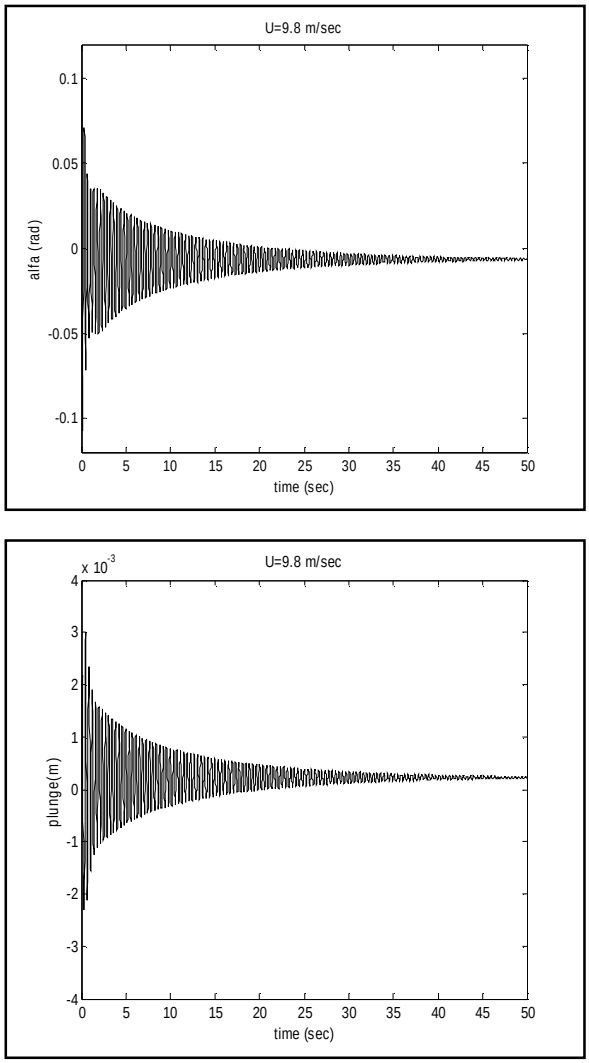

Fig.2. Time history of Pitch Angle and Plunging At 9.8 M/S Speed and Initial Conditions ($h(0) = 0; a(0) = 0.1rad$ **).**

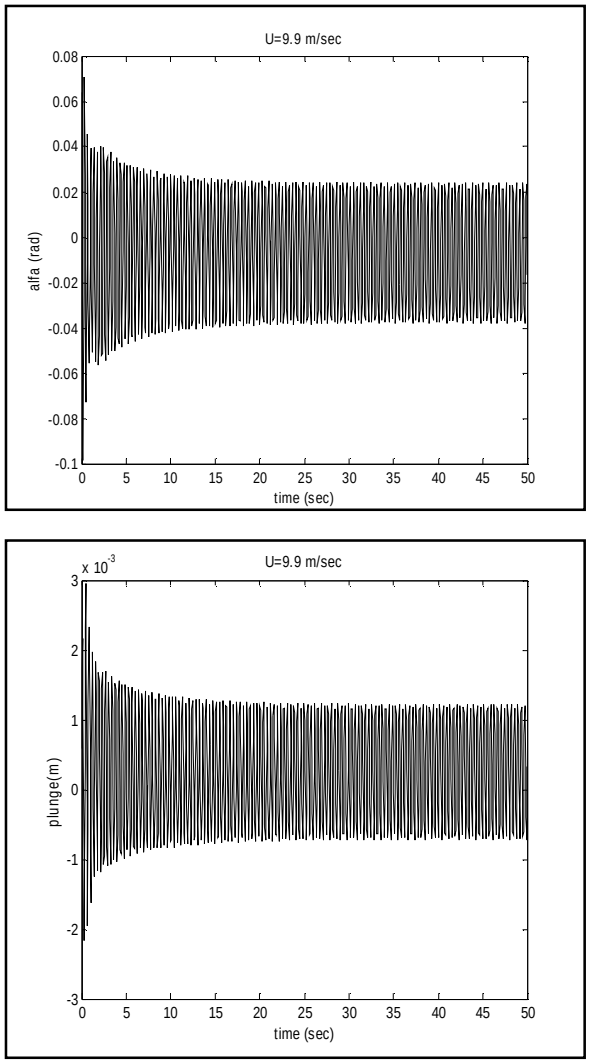

Fig.3. Time History of Pitch Angle and Plunging at 9.9 M/S Speed and Initial Conditions () $h(0) = 0; a(0) = 0.1rad$.

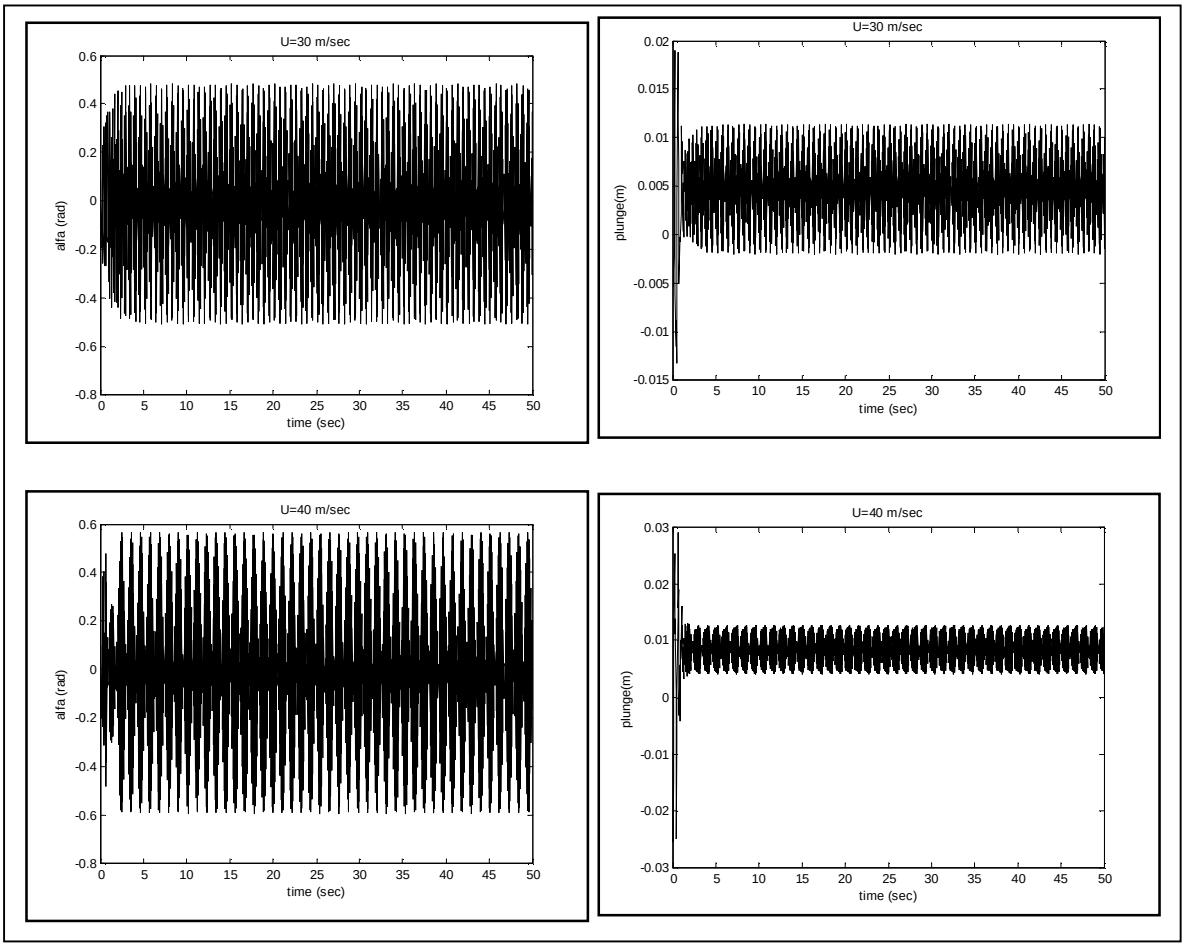

Fig.4. Time History of Pitch Angle and Plunging at 30m/s and 40m/sec Speed With Initial Conditions ($h(0) = 0; a(0) = 0.1rad$).

2.3. Adaptive Nonlinear Neural Control Methodology

The approach to control wing motion depends on the available information about the system and the control objectives. The 2-D wing system is considered as modified Elman recurrent neural networks model. The first step in the procedure of the control structure is the identification of nonlinear dynamics of 2-D wing system from the input-output data. Then a feed forward neural controller is designed using feed forward multi-layer perceptron neural network to find flap angles that control the plunge and pitching wing motion.

The proposed structure of the adaptive nonlinear neural controller can be given in the form of block diagram as shown in figure (5). It consists of:

1- Neural Network Identifier of 2-D wing system .
2- Feed forward Neural Controller.

In the following sections, each part of the proposed controller will be explained in details.

2.4. Nonlinear 2-D Wing System Neural Network Identifier

The modified Elman recurrent neural network model is applied to construct the 2-D wing system neural network identifier as shown in figure (5). The nodes of input, context, hidden and output layers are highlighted. The network uses two configuration models, series-parallel and parallel identification structures, which are trained using dynamic back-propagation algorithm.

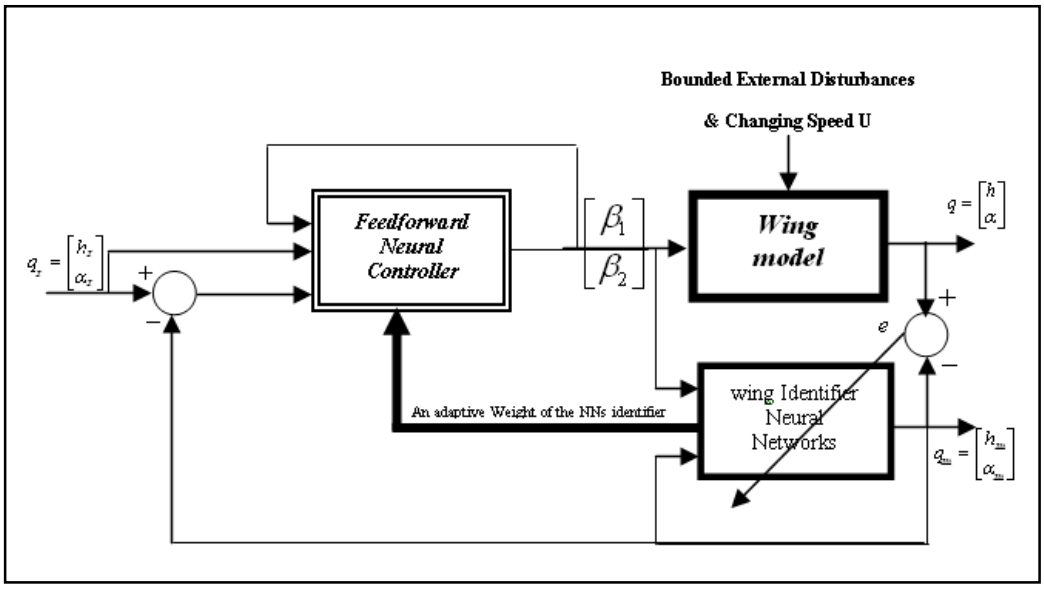

Fig.5. The Proposed Structure of the Adaptive Nonlinear Neural Controller for the 2-D Wing .

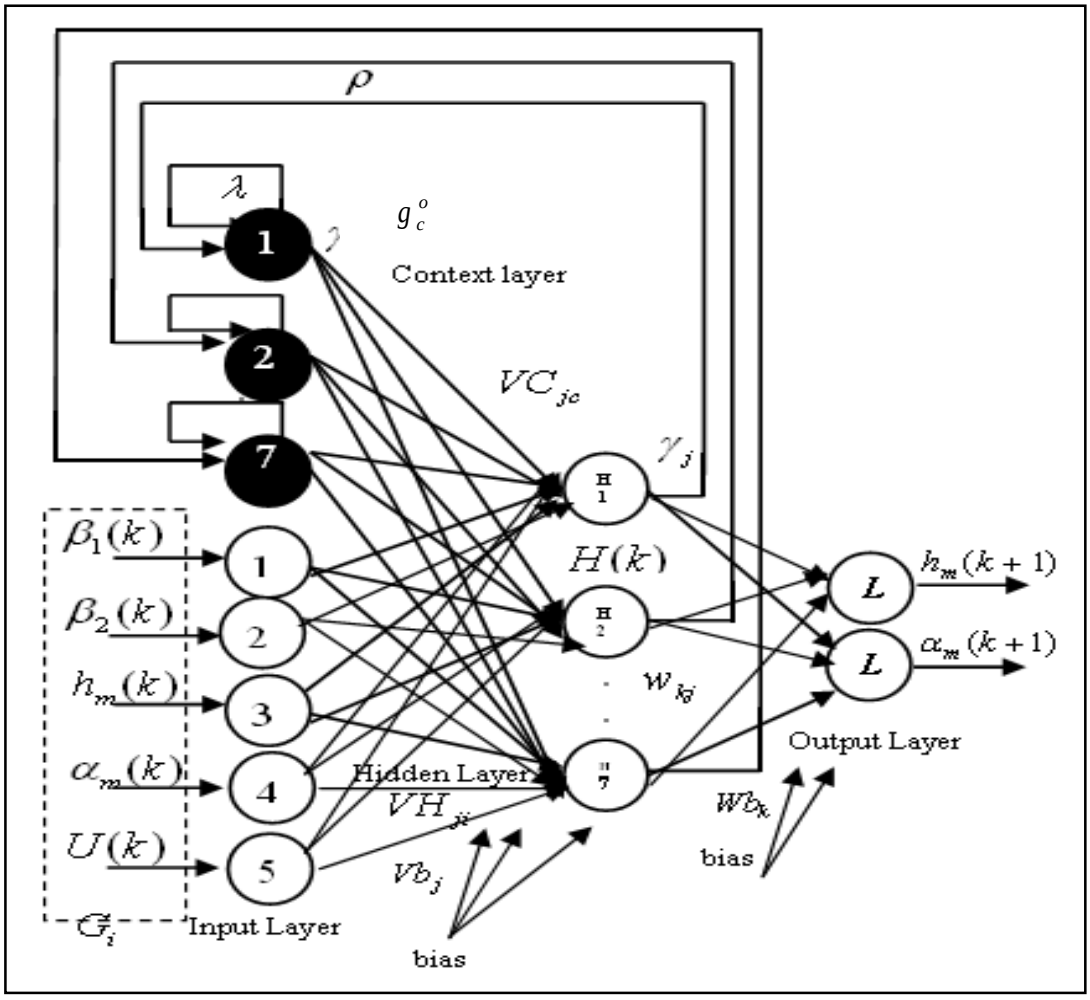

Fig.6. The Modified Elman Recurrent Neural Networks Acts as the Plunging and Pitch Motion of the Wing.

The structure shown in figure (6) is based on the following equations:

$$g(k) = F\{VH\overline{G}(k), VC\overline{g^{o}}(k), bias\overline{Vb}\} \quad \ldots(6)$$

$$O(k) = (Wg(k), bias\overline{Wb}) \quad \ldots(7)$$

where *VH*,*VC* and *W* are weight matrices, $\overline{Vb}$ and $\overline{Wb}$ are weight vectors and *F* is a non-linear vector function. The multi-layered modified Elman neural network, shown in figure (7), is composed of many interconnected processing units called neurons or nodes. The network weights are denoted as follows:

VH :Weight matrix of the hidden layers.
VC : Weight matrix of the context layers.
$\overline{Vb}$: Weight vector of the hidden layers.
W : Weight matrix of the output layer.
$\overline{Wb}$: Weight vector of the output layer.
L : Denotes linear node.
H : Denotes nonlinear node with sigmoidal function.

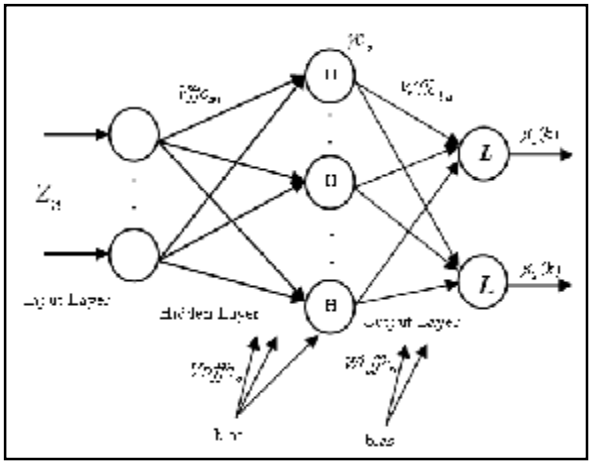

Fig.7. The Multi-Layer Perceptron Neural Networks of the Feed forward Neural Controller.

In order to improve the ability of network memory, self-connections, with fixed value l , are introduced into the context units of the network to give these units a certain amount of inertia [13]. The introduction of self-connections in the context units increases the possibility of modelling high-order systems by Elman network.
The output of the context unit in the modified Elman network is given by:

$$g_c^{o}(k) = l\, g_c^{o}(k-1) + r\, g_c(k-1) \quad \ldots(8)$$

where $g_c^{o}(k)$ and $g_c(k)$ are the outputs of the context and hidden units respectively. l is the feedback gain of the self-connections and r is the connection weight from the hidden units (j^{th}) to the context units (c^{th}) at the context layer. The value of l and r are selected randomly between (0 and 1) [13] . To explain these calculations, consider the general j^{th} neuron in the hidden layer. The inputs to this neuron consist of an i–dimensional vector, where i is the number of the input nodes. Each of the inputs has *VH* and *VC* weights associated with it.
$\overline{Vb}$ is the weight vector for the bias input set equal to -1 to prevent the neurons quiescent. The first calculation within the neuron consists of calculating the weighted sum net_j of the inputs as [13 and 14]:

$$net_j = \sum_{i=1}^{nh} VH_{ji} \times G_i + \sum_{c=1}^{C} VC_{jc} \times g_c^{o} + bias \times Vb_j \quad \ldots(9)$$

Where *j*.is the number of the hidden nodes, c is the number of the context nodes and $\overline{G}$ is the input vector. The outputs of the identifier are the modelling plunge and pitch motion and are defined as: $q_m = (h_m, a_m)^T$
where
h_m : plunge motion of the wing identifier.
a_m Pitch motion of the wing identifier.

The learning algorithm will be used to adjust the weights of dynamical recurrent neural network. Dynamic back propagation algorithm is used to train the Elman network. The sum of the square of the differences between the desired outputs $q = (h, a)^T$ and neural network identifier outputs $q_m = (h_m, a_m)^T$ is given by equation (10).

$$E = \frac{1}{2}\sum_{i=1}^{np}((h-h_m)^2 + (a-a_m)^2) \quad \ldots(10)$$

where *np* is the number of patterns.

The connection matrix between hidden layer and output layer is W_{kj}

$$\Delta W_{kj}(k+1) = -h\frac{\partial E}{\partial W_{kj}} \quad \ldots(11)$$

where h is the learning rate.

$$\frac{\partial E}{\partial W_{kj}} = \frac{\partial E}{\partial q_m(k+1)}\frac{\partial q_m(k+1)}{\partial o_k}\frac{\partial o_k}{\partial net_k}\frac{\partial net_k}{\partial W_{kj}} \quad \ldots(12)$$

$$\Delta W_{kj}(k+1) = h \times g_j \times e_k \quad \ldots(13)$$

$$W_{kj}(k+1) = W_{kj}(k) + \Delta W_{kj}(k+1) \quad \ldots(14)$$

The connection matrix between the input layer and hidden layer is VH_{ji}

$$\Delta VH_{ji}(k+1) = -h\frac{\partial E}{\partial VH_{ji}} \quad \ldots(15)$$

$$\frac{\partial E}{\partial VH_{ji}} = \frac{\partial E}{\partial q_m(k+1)}\frac{\partial q_m(k+1)}{\partial o_k}\frac{\partial o_k}{\partial net_k}\frac{\partial net_k}{\partial g_j}\frac{\partial g_j}{\partial net_j}\frac{\partial net_j}{\partial VH_{ji}} \quad \ldots(16)$$

$$\Delta VH_{ji}(k+1) = h \times f(net_j)' \times G_i \sum_{k=1}^{K} e_k W_{kj} \quad \ldots(17)$$

$$VH_{ji}(k+1) = VH_{ji}(k) + \Delta VH_{ji}(k+1) \quad \ldots(18)$$

The connection matrix between context layer and hidden layer is VC_{ji}

$$\Delta VC_{jc}(k+1) = -h\frac{\partial E}{\partial VC_{jc}} \quad \ldots(19)$$

$$\frac{\partial E}{\partial VC_{jc}} = \frac{\partial E}{\partial q_m(k+1)}\frac{\partial q_m(k+1)}{\partial o_k}\frac{\partial o_k}{\partial net_k}\frac{\partial net_k}{\partial g_j}\frac{\partial g_j}{\partial net_c}\frac{\partial net_c}{\partial VC_{jc}} \quad \ldots(20)$$

$$\Delta VC_{jc}(k+1) = h \times f(net_j)' \times g_c^o \sum_{k=1}^{K} e_k W_{kj} \quad \ldots(21)$$

$$VC_{jc}(k+1) = VC_{jc}(k) + \Delta VC_{jc}(k+1) \quad \ldots(22)$$

2.5. Feed Forward Neural Controller

The Feed Forward Neural Controller (FFNC) is essential to stabilize the tracking error of the wing system when the response of the wing is drifted from the desired condition during transient state and kept the steady-state tracking error at zero. The controller generates flap angles $b_1(k)$ and $b_2(k)$ control action that minimizes the cumulative error between the desired condition and the output response of the wing. The FFNC is supposed to learn the adaptive inverse model of the wing with off-line and on-line stages to calculate wing's reference input flap angle and keep the wing stable without flutter state in the presence of any disturbances or dynamics parameters changing.

To achieve FFNC, a multi-layer Perceptron model is used as shown in figure (7). The network notations are as follows:

$Vffc$: Weight matrix of the hidden layers.
$\overline{V}bffc$: Weight vector of the hidden layers.
$Wffc$: Weight matrix of the output layer.
$\overline{Wb}\,ffc$: Weight vector of the output layer.

To explain these calculations, consider the general a^{th} neuron in the hidden layer shown in figure (7.) The inputs to this neuron consist of an n–dimensional vector, where n is the number of the input nodes. Each input has an associated weight of $Vffc$. The first calculation within the neuron is to calculate the weighted sum of the inputs, $netc_a$ as [15, 16 and 17]:

$$netc_a = \sum_{a=1}^{nhc} Vffc_{an} \times Z_n + bias \times Vbffc_a \quad \ldots(23)$$

where *nhc* is the number of the hidden nodes.
Next, the output of the neuron h_a is calculated as the continuous sigmoid function of the $netc_a$ as:

$$gc_a = H(netc_a) \quad \ldots(24)$$

$$H(netc_a) = \frac{2}{1+e^{-netc_a}} - 1 \quad \ldots(25)$$

Once the outputs of the hidden layer have been calculated, they are passed to the output layer.

In the output layer, two linear neurons are used to calculate the weighted sum *netco* of its inputs, which are the output of the hidden layer as:

$$netco_b = \sum_{a=1}^{nhc} Wffc_{ba} \times gc_a + bias \times Wbffc_b \quad \ldots(26)$$

where $Wffc_{ba}$ are the weights between the hidden neuron gc_a and the output neurons. Then the sum ($netco_b$) will be passed through a linear activation function of slope 1; another slope can be used to scale the output, as:

$$Oc_b = L(netco_b) \quad \ldots(27)$$

The outputs of the feedforward neural network controller represent flap angles, $b_1(k)$ and $b_2(k)$.

The training of the feedforward neural controller is performed off-line as shown in figure (8). And adaptive weights are adapted on-line. It depends on the posture neural network identifier to find the wing Jacobian through the neural identifier model. This approach is currently considered as one of the better approaches that can be followed to overcome the lack of initial knowledge.

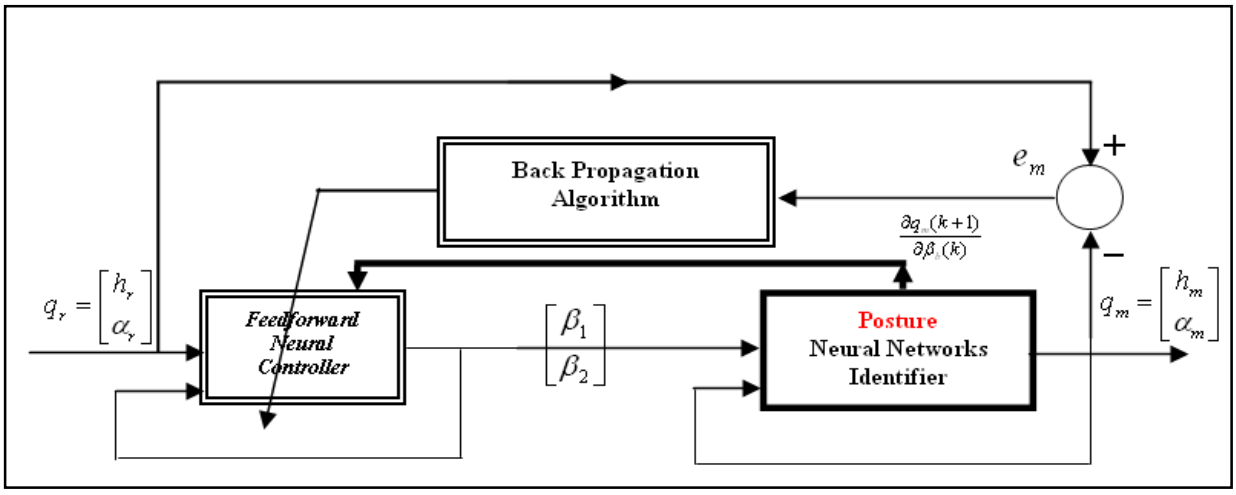

Fig.8. The Structure of the Feed forward Neural Controller for Wing Model.

The dynamic back propagation algorithm is employed to realize the training the weights of the feedforward neural controller. The sum of the square of the differences between the desired posture $q_r = (h_r, a_r)^T$ and neural network posture $q_m = (h_m, a_m)^T$ is:

$$Ec = \frac{1}{2}\sum_{i=1}^{npc}((h_r - h_m)^2 + (a_r - a_m)^2) \quad \ldots(28)$$

where *npc* is the number of patterns.

To achieve equation (28) a modified Elman neural network will be used as posture identifier. This task is carried out using an identification technique based on series-parallel and parallel configuration with two stages to learn the posture identifier. The first stage is an off-line identification, while the second stage is an on-line modification of the weights of the obtained wing neural identifier. The on-line modifications are necessary to keep tracking any possible variation in the dynamic parameters of the 2-D wing system. Back Propagation Algorithm (BPA) is used to adjust the weights of the posture neural identifier to learn dynamic of the 2-D wing system by applying a simple gradient decent rule.

The connection matrix between the hidden layer and the output layer is $Wcont_{ba}$

$$\Delta Wffc_{ba}(k+1) = -h\frac{\partial Ec}{\partial Wffc_{ba}} \quad \ldots(29)$$

$$\frac{\partial Ec}{\partial Wffc_{ba}} = \frac{\partial Ec}{\partial q_m(k+1)}\frac{\partial q_m(k+1)}{\partial b_b(k)}\frac{\partial b_b(k)}{\partial oc_b}\frac{\partial oc_b}{\partial netc_b}\frac{\partial netc_b}{\partial Wffc_{ba}} \quad \ldots(30)$$

$$\frac{\partial Ec}{\partial Wffc_{ba}} = \frac{\partial Ec}{\partial q_m(k+1)}\frac{\partial q_m(k+1)}{\partial b_b(k)}\frac{\partial b_b(k)}{\partial oc_b} f'(netc_b) gc_a \quad \ldots(31)$$

$$\frac{\partial Ec}{\partial q_m(k+1)} = \frac{\partial \frac{1}{2}\sum((h_r - h_m)^2 + (a_r - a_m)^2)}{\partial q_m(k+1)} \quad \ldots(32)$$

$$Jacobian = \frac{\partial q_m(k+1)}{\partial b_b(k)} \quad \ldots(33)$$

$$\frac{\partial q_m(k+1)}{\partial b_b(k)} = \frac{\partial q_m(k+1)}{\partial o_k(k)}\frac{\partial o_k(k)}{\partial net_k}\frac{\partial net_k}{\partial g_j}\frac{\partial g_j}{\partial net_j}\frac{\partial net_j}{\partial b_b(k)} \quad \ldots(34)$$

For linear activation function in the outputs layer:

$$\frac{\partial q_m(k+1)}{\partial b_b(k)} = \frac{\partial net_k}{\partial g_j}\frac{\partial g_j}{\partial net_j}\frac{\partial net_j}{\partial b_b(k)} \quad \ldots(35)$$

For nonlinear activation function in the hidden layer:

$$\frac{\partial q_m(k+1)}{\partial b_b(k)} = \sum_{k=1}^{K} W_{kj} f(net_j)'\frac{\partial net_j}{\partial b_b(k)} \quad \ldots(36)$$

$$\frac{\partial q_m(k+1)}{\partial b_b(k)} = \sum_{j=1}^{nh} f(net_j)'VH_{jb}\sum_{k=1}^{K} W_{kj} \quad \ldots(37)$$

Substituting equations (32 and 37) into equation (31), $\Delta Wffc_{ba}(k+1)$ becomes:

$$\Delta Wffc_{ba}(k+1) = hgc_a \times \sum_{j=1}^{nh} f(net_j)'VH_{jb}((eh_m(k+1)W_{1j}) + (ea_m(k+1)W_{2j})) \quad \ldots(38)$$

$$Wffc_{ba}(k+1) = Wffc_{ba}(k) + \Delta Wffc_{ba}(k+1) \quad \ldots(39)$$

The connection matrix between the input layer and the hidden layer is $Vffc_{an}$

$$\Delta Vffc_{an}(k+1) = -h\frac{\partial Ec}{\partial Vffc_{an}} \quad \ldots(40)$$

$$\frac{\partial Ec}{\partial Vffc_{an}} = \frac{\partial Ec}{\partial b_b(k)} \times \frac{\partial b_b(k)}{\partial oc_b} \times \frac{\partial oc_b}{\partial netc_b} \times \frac{\partial netc_b}{\partial gc_a} \times \frac{\partial gc_a}{\partial netc_a} \times \frac{\partial netc_a}{\partial Vffc_{an}} \quad \ldots(41)$$

$$\frac{\partial Ec}{\partial Vffc_{an}} = \frac{\partial Ec}{\partial q_m(k+1)} \frac{\partial q_m(k+1)}{\partial b_b(k)} \frac{\partial b_b(k)}{\partial oc_b} \times \frac{\partial oc_b}{\partial netc_b} \times \frac{\partial netc_b}{\partial gc_a} \times \frac{\partial gc_a}{\partial netc_a} \times \frac{\partial netc_a}{\partial Vffc_{an}} \quad \ldots(42)$$

$$\frac{\partial Ec}{\partial Vffc_{an}} = \frac{\partial Ec}{\partial q_m(k+1)} \frac{\partial q_m(k+1)}{\partial b_b(k)} \times \sum_{b=1}^{B} Wffc_{ba} \times f(netc_a)' \times Z_n \quad \ldots(43)$$

Substituting equations (32 and 37) into equation (43), $\Delta Vffc_{an}(k+1)$ becomes:

$$\Delta Vffc_{an}(k+1) = hZ_n f(netc_a)' \sum_{b=1}^{B} Wffc_{ba} \sum_{j=1}^{nh} f(net_j)' \sum_{i=1}^{I} VH_{ji}((eh_m(k+1)W_{1j}) + (ea_m(k+1)W_{2j})) \quad \ldots(44)$$

The B and I are equal to two because there are two outputs in the feedforward neural controller.

$$Vffct_{an}(k+1) = Vffc_{an}(k) + \Delta Vffc_{an}(k+1) \quad \ldots(45)$$

Once the feedforward neural controller has learned, it generates the flap control action to keep the output of the wing at reference value and to overcome any external disturbances during motion.

3. Results and Discussion

The proposed controller is verified with computer simulation using C++ program. The dynamics model of 2-D wing system described in section 2 is used. The simulation is carried out by tracking a desired plunging and pitch angle during flutter or limit cycle oscillation condition. The parameter values of a two Degree Of Freedom (2-DOF) airfoil system (typical section model) are taken from [5] see table (1).

The fist stage of operation is to set the position (plunging motion) and orientation about the elastic axis (pitch angle) neural network identifier. This task is performed using series-parallel and parallel identification technique configuration with modified Elman recurrent neural networks model. The identification scheme of the nonlinear MIMO (2-DOF) airfoil system are needed to input-output training data pattern to provide enough information about dynamics (2-DOF) wing model to be modelled. This can be achieved by injecting a sufficiently rich input signal to excite all process modes of interest while also ensuring that the training patterns adequately covers the specified operating region. A hybrid excitation signal has been used for the 2-D wing model. Figure (9) show the input signals $b_1(k)$ and $b_2(k)$,.

Table 1,
System Parameters [5]

b	0.135 m
d	-0.45
m	12.387 kg
x_a	0.25
I	0.065 kg.m^2
k_h	2844.4 N/m
$k_\alpha(\alpha)$	12.77+53.47α+1003α^2 N/rad [11]
c_h	27.43
c_α	0.036
ρ	1.225 kg/m^3
$C_{L\alpha}$	6.28
$C_{m\alpha}$	-0.635
$C_{L\beta1}$	3.358
$C_{L\beta2}$	3.458
$C_{m\beta1}$	-0.635
$C_{m\beta2}$	-0.735

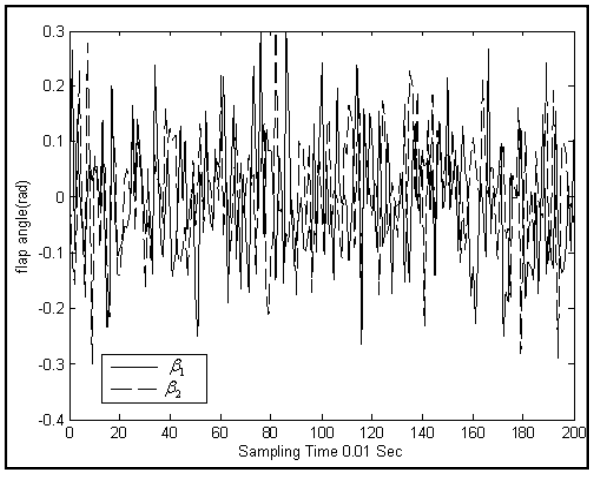

Fig.9. The PRBS Input Flap Angles Signals Used to Excite the Wing Model.

The training set is generated by feeding a Pseudo Random Binary Sequence (PRBS) signals, to the model and measuring its corresponding outputs, position (plunging motion) and orientation (pitch angle), with a sampling time of 0.01 second. This value was found adequate for the stability and convergence of solution. Back propagation learning algorithm is used with the modified Elman recurrent neural network of the structure 5-7-7-2. The number of nodes in the input, hidden, context and output layers are 5, 7, 7 and 2 respectively as shown in figure (6).

A training set of 200 patterns has been used with a learning rate of 0.1 and variable speed inputs U=[25, 30, 35, 40 and 45] m/sec. After 5439 epochs, the identifier outputs of the neural network, position (plunge motion) and orientation about (pitch angle), are approximated to the actual outputs as shown in figure (10). The objective cost function MSE is less than 16×10^{-5} as shown in figure (11).

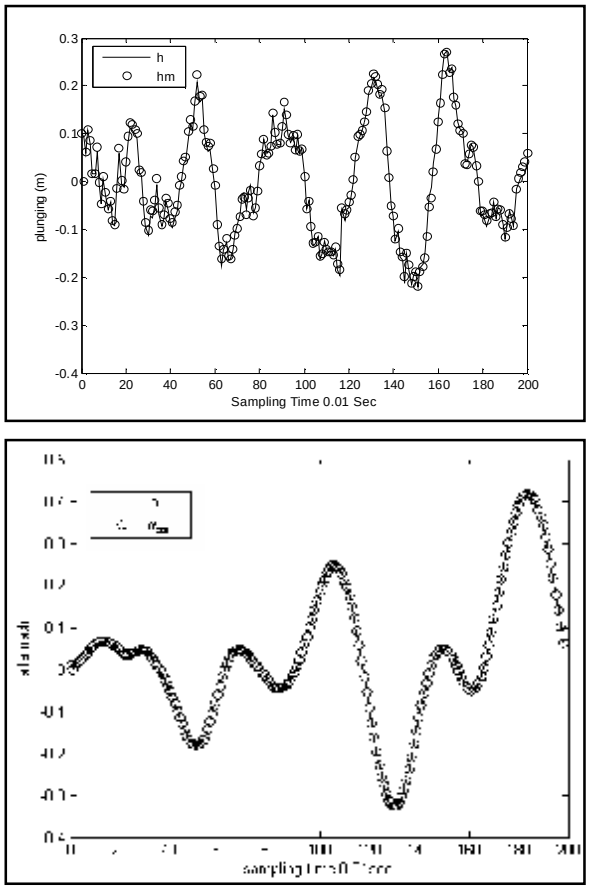

Fig.10. The Response of the Neural Network Identifier with the Actual 2-D Wing Model Output for the Learning Set.

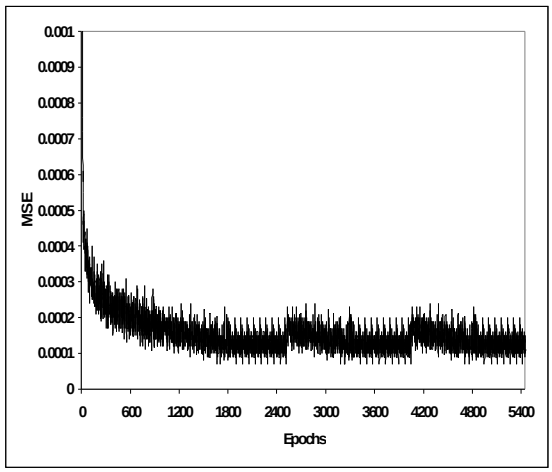

Fig.11. The MSE of the Cost function.

Parallel configuration is used to guarantee the similarity between the outputs of the neural network identifier and the actual outputs of the plunging motion and pitch angle of the wing. At 3859 epochs the same training set patterns has been achieved with an MSE less than 1.9×10^{-6}.

The testing set is generated by difference feeding a PRBS signals as shown in figure (12), and it is applied to the system.

Figure (13) compare the time response of the parallel mode output with the actual plant output, and there is excellent identification.

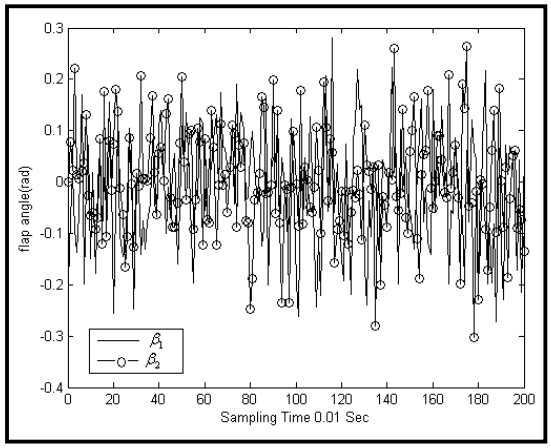

Fig.12. The PRBS Input Flap Angles Signals Used for Testing 2-D Wing Identifier Model.

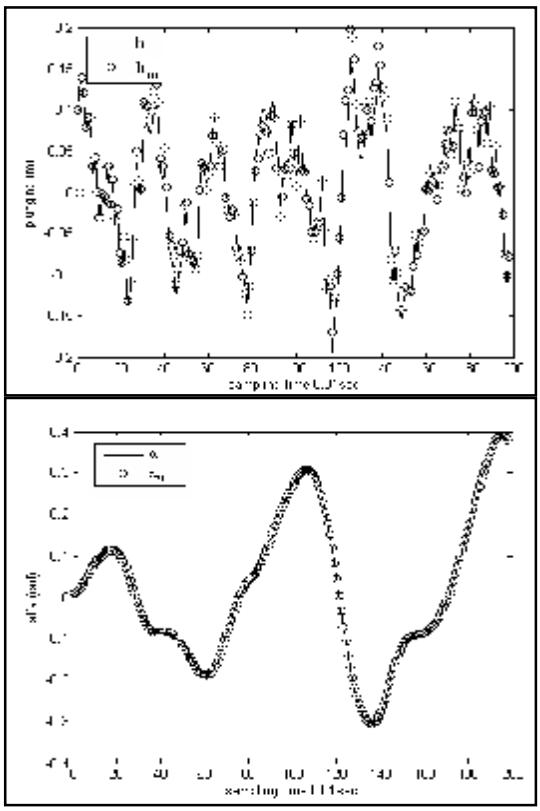

Fig.13. The Response of the Neural Network Identifier with the Actual 2-D Wing Model Output for the Testing Set.

The final stage of the proposed controller is feedforward neural controller. It uses multi-layer perceptron neural network 6-13-2 as shown in figure (7). The desired conditions has been learned by the feedforward neural controller with off-line and on-line adaptation stages using back propagation algorithm as shown in figure (8) to find the suitable control action.

The controller performance is simulated at three values of the flight speed (30, 35, 45 m/sec) in unstable region and at different initial conditions of plunging motion and pitch angle. Figure (14) shows the closed loop responses for the controlled 2-D wing system. The controller reach the requirements and the closed-loop simulation obtained is stable .The over shoot and settling time increase slightly with the increasing of the velocity. Also the oscillation during the transient period appears with the increasing of the velocities, but its amplitude is small and converge of desired condition is quick with settling time 0.4sec at high velocity *U=40m/sec*.

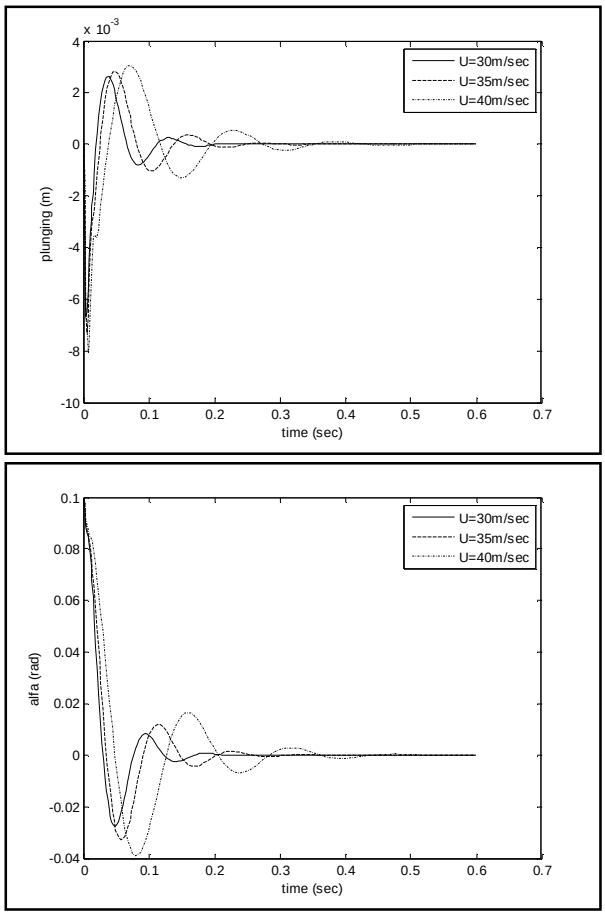

Fig.14. System Responses with Controller at Different Speed and Initial Conditions $(h(0)=0; a(0)=0.1rad)$.

In figure (15) the responses of the controller effort (flap angles) at U=30m/sec and 40m/sec are shown. It is clear that the control action β_1 has large values in comparing with another control action β_2 .Also the control actions never exceed ± 0.3 rad. The values of flap angles are limited from -0.3 to 0.3 rad. to make the controller works in logical limits.

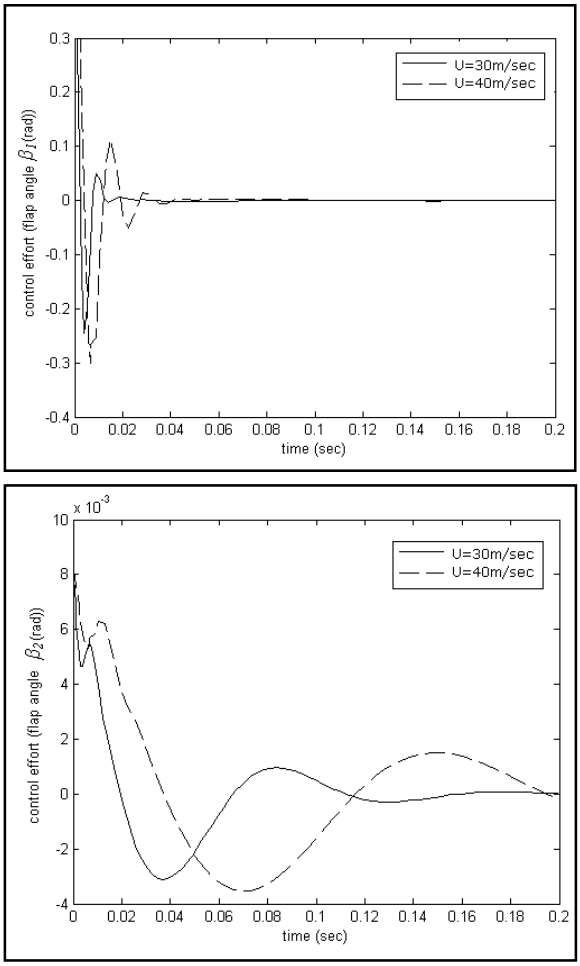

Fig.15. Control Efforts at Different Speed and Initial Conditions $(h(0)=0; a(0)=0.1rad)$.

The values of the initial conditions are varying to make the nonlinear stable or unstable, so the present controller performance is tested at different initial conditions as shown in figure (16). When the initial values of plunging and pitch angle increase the over shoot and the oscillation increase during the transient period. The plunging initial value has large effect on the responses than pitch angle initial value. But the present controller can give acceptable performance and reaches to desired condition at very short settling time about 0.2sec. This result compares very well with reference [5].

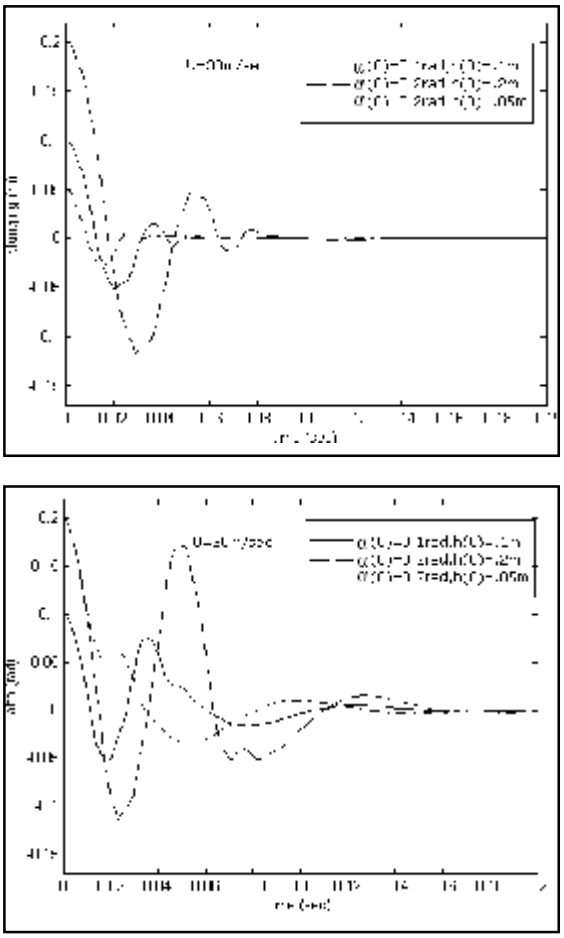

Fig.16. System Responses with Controller at Different Initial Conditions.

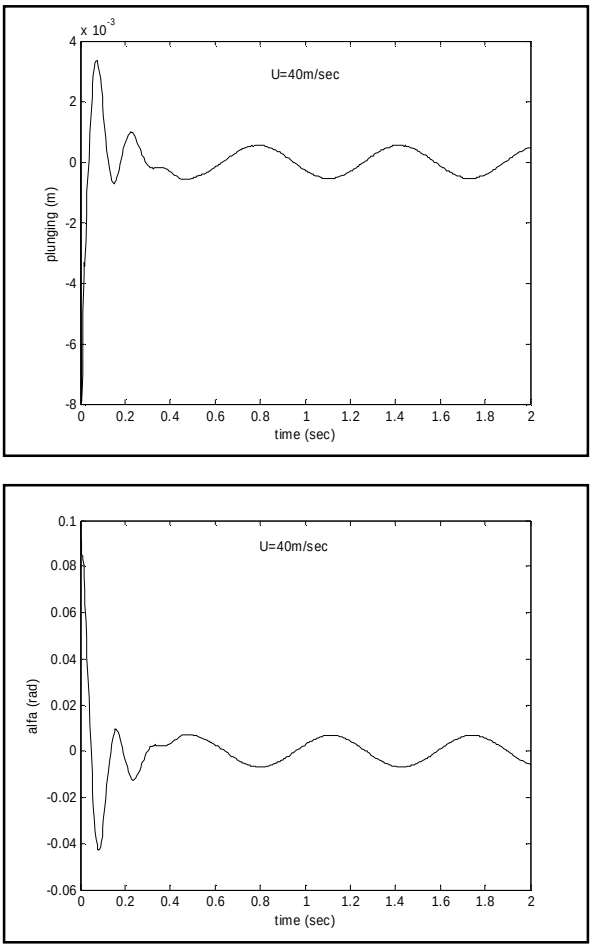

Fig.17. System Responses with Sinusoid Disturbanceat initial Conditions $(h(0) = 0; a(0) = 0.1rad)$.

Finally, to investigate the present controller performance at difficult conditions, the disturbance action is introduced on the wing model at high velocity *U=40m/sec*. In figure (17) the responses of controller with sinusoid disturbance has been shown. The amplitude of disturbance is taken as 300% the maximum values of control actions and frequency 10 Hz. In spite of the existence of bounded disturbances the adaptive learning and robustness of neural controller show small effect of these disturbances. The controller achieves the desired condition with very small fluctuation. For plunging and pitch motions the fluctuation was 0.00055 m and 0.0068 rad. respectively. These values are less than the maximum fluctuation for the same wing section [18] (about 0.048*b* for plunging and 0.024 rad. for pitch motion).

4. Conclusions

In the current work, it has been shown that the proposed controller has the capability to generate smooth and suitable flap commands, b_1 and b_2 without sharp spikes. Moreover, it has the capability of effectively eradicating the tracking errors for the 2-D wing model. The principal conclusions may be summarized as follows:

- Excellent identification is achieved when comparing the time response of the parallel mode output with the actual plant output.
- The controller reach the requirements and the closed-loop simulation obtained is stable. The over-shoot and settling time increase slightly with the velocity. The amplitude of oscillation during the transient period is small and converge to desired condition.
- The controller worked in logical limits, the control action never exceeds ± 0.3 rad.
- The plunging initial value has large effect on the response than pitch angle initial value.
- Simulation results show that the proposed controller is robust and effective in comparison with the controller in [5] in terms of fast response with minimum settling times and minimum

tracking error despite the presence of bounded external disturbances.

5. References

[1] Shams Sh., Sadr M.H.,and Haddadpour H. " Nonlinear aeroelastic response of slender wings based on Wagner function", Thin-Walled Structures ,Vol 46 (2008) pp.1192–1203

[2] Woolston DS, Runyan HL,and Andrews RE. "An investigation of certain types of structural nonlinearities on wing and control surface flutter" J Aeronaut Sci, Vol 24,(1957),pp.57–63.

[3] Frampton, K.D., and Clark, R.L. "Experiments on control of limit cycle oscillations in a typical section" , AIAA Paper 99-1466'. Proc.40th Structures, Structural Dynamics and Material Conf., St. Louis, MO, (1999), pp. 2195–2055

[4] Palaniappan K, Sahu P.and Alonso J.J " Design of Adjoint Based Laws for wing flutter control",American Institute of Aeronautics and Astronautics Paper AIAA-(2009)-148.

[5] Afkhami S. and . Alighanbari H. "Nonlinear control design of an airfoil with active flutter suppression in the presence of disturbance", IET Control Theory Appl., Vol. 1, No. 6, November (2007)

[6] Haiwei, Y. and Jinglong H. " Robust flutter analysis of a nonlinear aeroelastic system with parametric uncertainties", Aerospace Science and Technology , Vol 13 ,(2009) pp.139–149

[7] Zeng, Y., and Singh, S.N "Output feedback variable structure adaptive control of an aeroelastic system", J. Guidance Control Dyn.,Vol 21, (1998), pp. 830–837

[8] Melin P.and Castillo O." Adaptive intelligent control of aircraft systems with a hybrid approach combining neural networks, fuzzy logic and fractal theory", Applied Soft Computing vol3, (2003) pp.353–362

[9] Chen C., Wu J.and Chen J. " Prediction of flutter derivatives by artificial neural networks", Journal of Wind Engineering and Industrial Aerodynamics ,Vol. 96 ,(2008), pp.1925–1937

[10] Demenkov M. "Form Local to Global Stabilizility of Aeroelastic oscillation",18th IEEE International Conference on Control Apllictions ,Saint Petersburg ,Russia, 2009.

[11] Abbas1 L K, Chen1 Q. and Milanese A. " Non-linear aeroelastic investigations of store(s)-induced limit cycle oscillations", J. Aerospace Engineering Vol. 222 Part G (2008).

[12] Ogata K.Modern Control Engineering, Prentice-Hall International.Inc(1970)

[13] Pham D. T. and Xing L. " Neural Networks for Identification, Prediction and Control", Springer, (1995).

[14] S. Omatu, M. Khalid, and R. Yusof "Neuro-Control and its Applications" London: Springer-Velag, 1995.

[15] Zurada J. M., Introduction to Artificial Neural Systems. Jaico Publishing House, Pws Pub Co. (1992).

[16] K. S. Narendra and K. parthasarathy, "Identification and control of dynamical systems using neural networks," IEEE Trans. Neural Networks, vol. 1,pp. 4-27, 1990.

[17] K. S. Narendra and K. parthasarathy, "Gradient methods for the optimization of dynamical systems containing neural networks," IEEE Trans. Neural Networks, vol. 2 No. 2, pp. 252-262, 1991.

[18] Abu-Tabikh,M.I." Modeling of Steady and Unsteady Tturblunent Boundary Layer Separation Using Vortex Hybrid Method ", Ph.D thesis, Department of Mechanical Engineering, U.O.T, Baghdad,1997.

السيطرة على رفرفة جناح ثنائي الأبعاد باستخدام مسيطر عصبي لا خطي متكيف

د. موفق علي توفيق* **د. محمد إدريس محسن*** **حيدر صباح عبد الأمير****

* قسم هندسة المكائن والمعدات/ الجامعة التكنولوجية

** قسم الهندسة الميكانيكية/ معهد التكنولوجيا - بغداد

الخلاصة

تم في هذا البحث اقتراح مسيطر عصبي لاخطي متكيف للسيطرة على الرفرفة لنموذج جناح ثنائي الأبعاد. تنشا المؤثرات اللاخطية في منظومة الجناح من النموذج الايروديناميي شبه المستقر والنابض ألالتوائي باتجاه التأرجح. تم تحديد المنطقة التي يكون فيها النظام غير مستقر من خلال فحص استجابته مع الزمن حيث تم إيجاد السرعة التي تبدأ عندها ظاهرة الرفرفة والتذبذب الدوري المحدد. تتكون هيكلية المسيطر من نموذجين هما الشبكة العصبية المحسنة لألمن(MENN) و بيرسبتون متعدد الطبقات (MLP) .لقد تم تأهيل النموذج (MENN) في مرحلتين هما مرحلة الخط المغلق ومرحلة الخط المفتوح لضمان تطابق مخرج النموذج العصبي مع مخرج منظومة الجناح وهو حركة التأرجحية والحركة العمودية لتكوين النموذج العصبي المعرف. تم تأهيل المسيطر العصبي الأمامي من خلال الخط المغلق ثم تم تحديث الأوزان لهذا المسيطر من خلال الخط المفتوح لإيجاد زاوية الخافقة المطلوبة التي تسيطر على حركة التأرجح والحركة العمودية.تم استخدام خوارزمية الانتشار الخلفي لتأهيل النموذجين. كانت نتائج المحاكاة لهذا المسيطر العصبي اللاخطي فعالة من خلال تقليل الرفرفة إلى صفر وبزمن استقرار مناسب مع وجود ضوضاء خارجية.